Thermo-mechanical limits of a magnetically driven fast-ion loss detector in the ASDEX Upgrade tokamak

J. Hidalgo-Salaverri[1,2,*], J. Gonzalez-Martin[1,2], J. Ayllon-Guerola[1,2], M. Garcia-Munoz[1,3], B. Sieglin[4], J. Galdon-Quiroga[3], D. Silvagni[4], E. Viezzer[1,3], J. Rueda-Rueda[1,3], T. Lunt[4], A. Herrmann[4] and the ASDEX Upgrade Team

[1] *Centro Nacional de Aceleradores (CNA), Universidad de Sevilla, CSIC, J. De Andalucía, Seville, Spain*
[2] *Department of Mechanical Engineering and Manufacturing, University of Seville, Seville, Spain*
[3] *Department of Atomic, Molecular and Nuclear Physics, University of Seville, Seville, Spain*
[4] *Max-Planck-Institut für Plasmaphysik, Garching, Germany*
E-mail: jhsalaverri@us.es

A real-time control system is being developed for a magnetically driven Fast-Ion Loss Detector (FILD) at the ASDEX Upgrade tokamak. The insertion of the diagnostic head will be adjusted in real-time to react to changes in the graphite head temperature, plasma position and appearance of MHD instabilities. The graphite probe head of the detector is exposed to an intense heat flux (located ~3 – 5 cm from separatrix). The control algorithm performance is constrained by: the graphite head sublimation temperature, the ultimate stress limit, the reaction time of the controller and the retraction time. In this work, the temperature and thermal induced stress distribution on the probe head are assessed to determine what temperature-related magnitude is the limiting factor.

The heat flux at the probe head has been estimated using the time-averaged parallel heat flux measured at the divertor target via infrared thermography. A field line tracing algorithm determines which regions of the probe head receives a weighted heat flux due to shadowing (self-induced or from other structures) and the incidence angle of the field lines. A finite element model is used to simulate the temporal evolution of the graphite head temperature and to obtain the induced thermal stress. The temperature spatial distribution at the probe head is validated against measurements of the probe head for different FILD systems showing a good agreement. These measurements have been obtained from visible cameras with an infrared filter. The model concludes that the maximum stress (~100 MPa) does not overcome the graphite mechanical limit (170 MPa) and that the probe head is not affected by fatigue. Therefore, the graphite sublimation temperature (2000ºC) is set as the limiting factor of the new control system.

KEYWORDS: fast-ions, fast-ion loss detector, thermo-mechanical analysis, finite elements analysis

* Corresponding author

1. **Introduction**

Fast-ions loss detectors (FILD) have been installed in several tokamaks [1]–[4] to diagnose the loss of these highly energetic particles [2], [5], [6]. These losses can, for example, reduce the efficiency of external heating systems like neutral beam injection (NBI) or ion cyclotron resonance heating (ICRH) and damage the plasma facing components [7]. In the ASDEX Upgrade tokamak, an array of FILDs provides time-resolved velocity-space measurements of the fast-ions population at different wall locations. One of these detectors (known as FILD4) is mounted in a magnetic drive and [8], [9] and can also provide radial measurements during a plasma discharge.

FILD systems are directly exposed to the plasma during their operation and, therefore, are exposed to a high heat flux [7], [10], [11]. For this magnetically driven FILD, a closed-loop real-time control system is being developed. The controller will optimise the measuring position of the detector considering the probe head temperature. The featured thermal model will set the upper operational temperature threshold. The goal of this work is to investigate if said threshold is determined by the sublimation temperature of the graphite probe head or by the induced thermo-mechanical stress.

In Section 2, the thermal model used to obtain the heat flux on the probe head is described. Section 3 introduces the characteristics of the built finite elements model. Section 4 uses the heat flux as the input for the finite elements model to determine if the limit of the graphite probe head comes from its sublimation temperature or from the induced thermal stress. Section 5 describes the conclusions of this work.

2. **Thermal model**

The heat flux profile at the divertor target is typically described by an exponential decay in the SOL region, which is parametrized by the e-folding length λ_q [12], [13]. Lunt et al. [14] propose a double exponential parametrization of the heat flux in the SOL, i.e., a shorter decay length that affects the near-SOL region and a longer one for the far-SOL. This double exponential fit shows better agreement with experimental data for plasma facing components in the far scrape-off layer as it is the case of the FILD systems.

$$q_{||} = q_{0,near} \cdot \exp\left(-s/\lambda_{q,near}\right) + q_{0,far} \cdot \exp\left(-s/\lambda_{q,far}\right) \quad (1)$$

Where q_0 is the parallel heat flux on the separatrix and λ_q the e-folding length for the near and far scrape-off layer exponential, respectively; s is the distance to the separatrix.

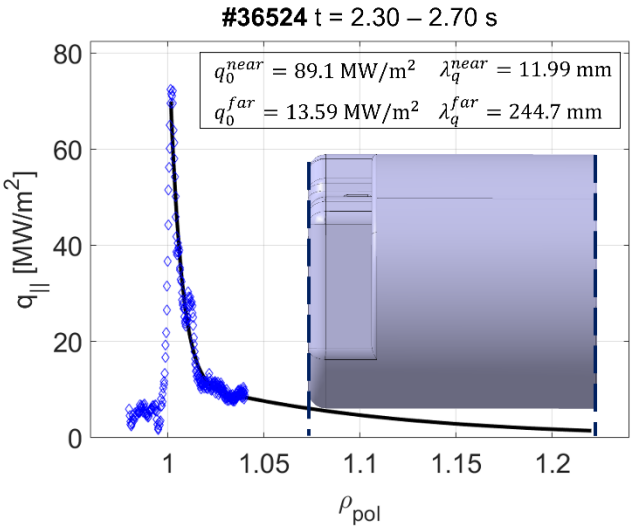

Figure 1. Parallel heat flux as a function of ρ_{pol}. The blue diamonds represent the experimental divertor datapoints and the black line is the double exponential fit. The position occupied by FILD4 in ρ_{pol} is also included.

Infrared cameras are used in the ASDEX Upgrade tokamak [15] to obtain the integrated perpendicular heat flux during a certain time period in the tungsten divertor tiles [16]. Equation 1 is particularized for the divertor region, to extend it to the complete first wall, the magnetic flux expansion must be taken into account, this is done by using the ρ_{pol} coordinate instead of s. Therefore, the double exponential fits the data in the $q_{||}$-s space and then it is translated to $q_{||}$-ρ_{pol}. Figure *1* shows the experimental data points, the fit and the position in ρ_{pol} occupied by FILD4 for shot #36524.

The heat flux on the probe head is obtained by multiplying the parallel heat flux by the cosine of the incident angle of the magnetic field lines with the probe head. Part of this heat flux may be shadowed by the surrounding structures. A magnetic field line tracer has been developed to consider said shadowing. If a field line can be traced back from the probe head uninterruptedly for a distance longer than the collection length [17] then that region can be considered as wet (it receives the totality of the heat flux). On the other hand, if the magnetic field line intersects with any structure before achieving the collection length, then that region will be considered as shadowed and will only receive a fraction of the heat flux. This is taken into account in the collection length correction factor, that is 1 when the surface is wet and the square ratio of the travelled distance over the collection length, when the surface is shadowed. Figure 2 shows the collection length correction factor and the estimated heat flux that gets to the probe head.

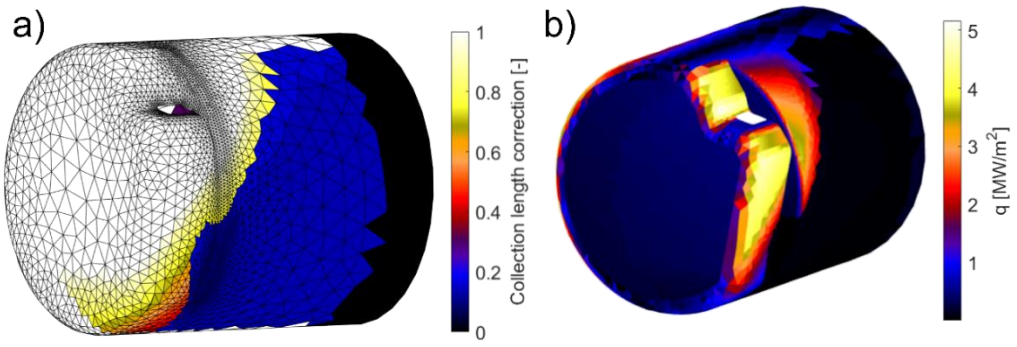

Figure 2. a) Collection length correction factor and b) heat flux over the FILD4 probe head for #36524 at 2.5 seconds.

3. **Finite elements analysis setup**

In this section, the setup for the thermal and mechanical simulations, as well as the used mesh are presented.

The Ansys software [18] has been used to perform a series of thermomechanical simulations of the probe head. Two models have been developed, one thermal (transient thermal) and one mechanical (static structural) and coupled together. The heat flux obtained in section 2 is used as the input, obtaining in return the temperature distribution and the related induced thermal stress during the experiment. In the thermal model, the probe head is considered as an isolated system with a fixed 25ºC temperature on its rear side. As the simulated time is short (< 10 seconds), heat will not be able to reach the rear side. This configuration has been tested against more realistic ones showing its convergency regardless of the boundary conditions employed on its rear surface. For the mechanical analysis, the probe head has been modelled with a fixed support in said rear side.

A convergency analysis for this model is depicted in Figure 3 b). The mesh has been refined with special care in areas where high temperature gradients or mechanical stresses where found, i.e., in the inner corners and in the thin regions (as in the hole region shown in Figure 3 a)). Figure 3 b) shows the evolution of the maximum temperature and maximum compression stress with the number of nodes used for the mesh. The maximum temperature converges considerably faster than the maximum stress, being already converged for < 10^5 nodes, as the mesh resolution is more relevant in the mechanical analysis than in the thermal system. On the other hand, the maximum stress requires a finer mesh,

getting to a stable solution after ~$2 \cdot 10^5$ nodes. The mesh is refined further to ensure that the corners and thin pieces are formed by, at least, three elements. This has no impact on the maximum temperature/stress that are the goal of this paper but ensures a well-converged system.

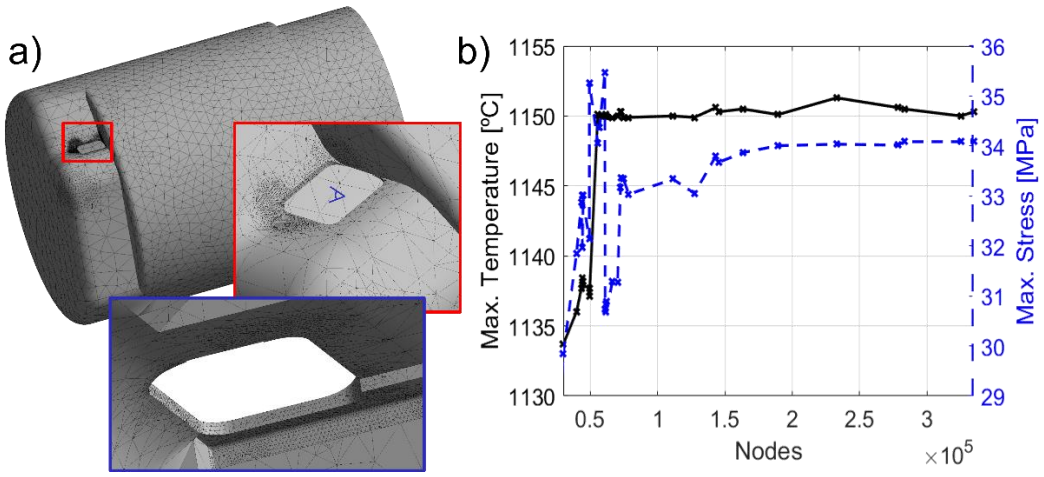

Figure 3. a) Mesh used for the finite elements simulations. In red, zoom on the exterior part of the hole where the finer mesh was required. In blue, detail of the interior part of the hole. b) Evolution of the maximum temperature and stress as the number of nodes of the mesh increases.

The FILD graphite probe head is manufactured on isostatically pressed graphite R6710. The material properties of this graphite are shown in Table 1. The used temperature-dependant properties are shown at 100ºC. In this table, the graphite thermo-mechanical limits are also shown, this is the sublimation temperature and its flexural/compressive strength. In this work, it is determined which one will set the upper temperature limit for the FILD systems. Knowing this limit is essential for the aforementioned real-time control system for FILD4 and to expand the operational window of all FILD systems.

Graphite isostatically pressed R6710			
Density	1880 kg/m^3	Specific heat (@ 100ºC)	895 J/kgK
Conductivity (@100ºC)	104.6 W/mK	Sublimation temperature [19]	2000ºC
Thermal expansion	$4.7 \cdot 10^6$ K^{-1}	Young's modulus	13.5 GPa
Flexural strength	85 MPa	Compressive strength	170 MPa

Table 1. Material properties and limits of the graphite probe head

4. **Thermo-mechanical assessment**

In this section, the heat flux obtained in section 2 is applied on the thermal finite elements model described on section 3. The goal of this model is to define the instant where the temperature on the probe head overcomes its sublimation temperature. For this, two scenarios are proposed, a real FILD4 trajectory and a more conservative scenario where the probe head is inserted at its maximum stroke for a long time (longer than the real duration of a FILD-compatible shot) until the temperature overcomes the sublimation threshold. These simulations have been carried out using the heat flux profile of shot #36524 that can be considered as a conservative FILD scenario in terms of the heat flux received by the probe head. The applied position-dependant heat flux has been obtained by averaging between 2.30 – 2.70 seconds.

Figure 4 shows the temperature and the equivalent von Misses stress evolution for the two discussed scenarios. The system receives a higher heat flux when fully inserted (Figure 4 a)) than when performing radial a scan (Figure 4 b)), therefore it will reach a higher temperature by the time the shot ends. Nonetheless, at the end of the shot in the former scenario, the probe head is still at ~1500ºC way lower than the sublimation limit of 2000ºC [19]. The sublimation temperature will not be reached until ~8 seconds, normally FILD operates up to 4 – 6 seconds. This simulation validates the safety approach of this operation strategy.

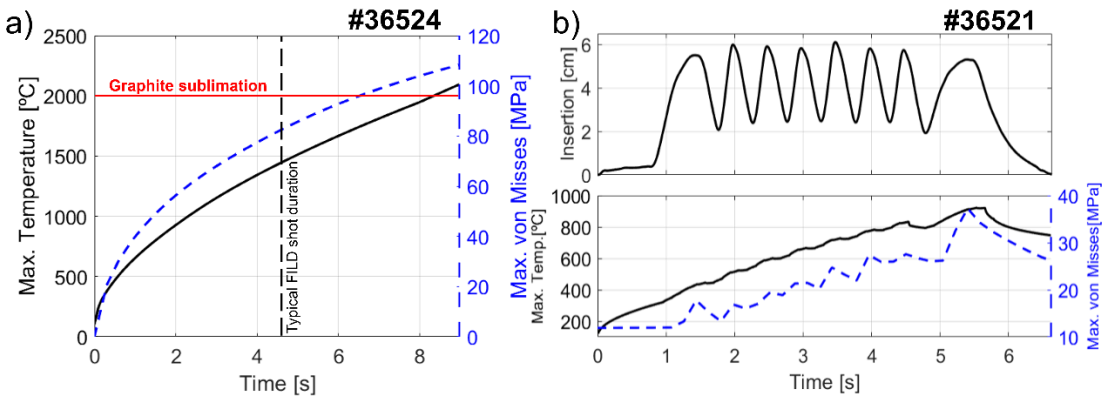

Figure 4. Temperature and equivalent von Misses stress evolution on the probe head. a) At maximum insertion for #36524 and b) performing a radial scan, calculated with shot #36521 real trajectory and #36524 conservative heat flux.

As expected, the probe head gets hotter every time the probe head goes to deeper insertions in the radial scan scenario. This scenario uses the trajectory performed by FILD4 in the shot #36521 with a typical heat flux. The insertion time trace used to determine the heat flux over the probe head during this scenario is shown in Figure 4 b). It is interesting to note that moving backwards from high insertions only significantly decreases the maximum temperature of the probe head if the reached temperature is high enough for the heat diffusion to overcome the received heat flux. On the other hand, the von Misses stress falls every time the probe head reduces its insertion as the temperature gradients over the probe head relax rapidly. This is important to take into account as the maximum stress may not be found at the moment of maximum temperature if the diffusion is dominant over the received heat flux. In the conservative case, as the high heat flux is constant the temperature gradients along the probe head only grow stepper over time and maximum stress coincides on time with the maximum temperature.

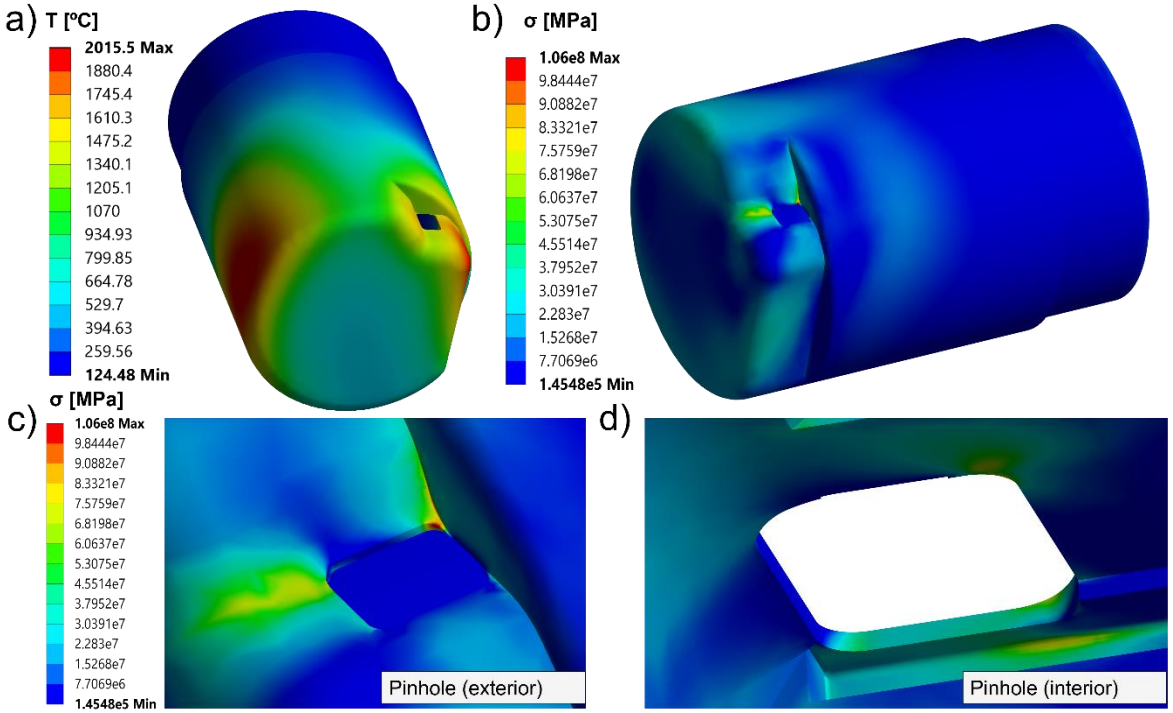

Figure 5 a), b) Temperature and equivalent von Misses stress distribution when sublimation is reached. Details of stress distribution in c) the exterior and d) inner part of the pinhole.

In the conservative scenario, by the time the sublimation temperature is reached the maximum von Misses stress (~100 MPa) is still well below the material limit (170 MPa). Therefore, the limiting factor on this device will be its temperature.

Figure 5 shows the temperature and equivalent von Misses stress distribution when the sublimation temperature is reached. The corner close to the hole reaches higher temperatures than the surrounding area and thus, it dilates more than the rest of the body. This leads to an important compression stress in the hole region specially in one of its inner corners and in the interior slot (used to accommodate the collimator). Even though, the induced stress is below its limit, these regions must be specially watched as part of the safety strategy of the detector.

This model has been validated against experimental measurements of the probe head temperature obtained with visible cameras with infrared filters [20]. Different FILD systems (namely FILD1, FILD4 and FILD5) have been compared, showing a nice qualitatively agreement on the temperature spatial distribution. Rodriguez et al. [11], show a similar experimental temperature distribution for the FILD1 system in another experiment. As the used thermal model does not compute the impact of fast ions, it cannot be used to get the absolute temperatures over time only the qualitative spatial distribution. Nonetheless, this is not the scope of this paper. The model does predict the temperature qualitative spatial distribution and can be used to determine which is the limiting factor for the FILD systems operation temperature.

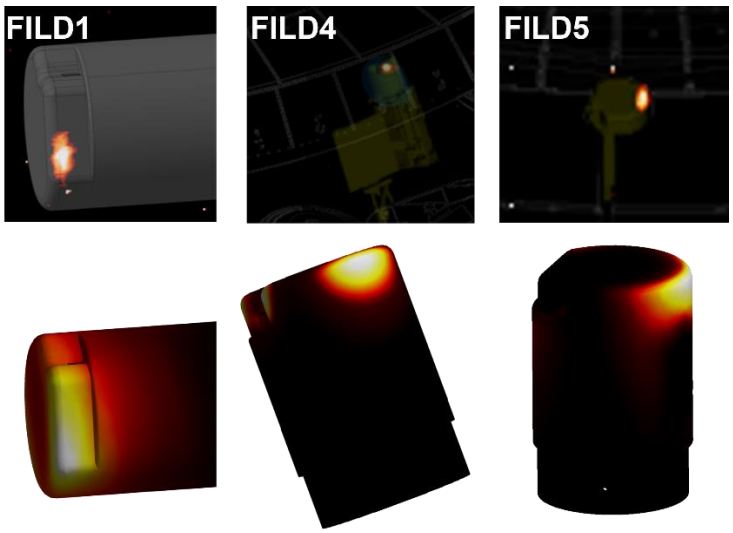

Figure 6. Qualitative spatial temperature distribution comparison between IR measurements and simulated scenarios for FILD1, FILD4 and FILD5.

The fatigue life of the detector has been conservatively addressed under the most extreme conditions. This is from the stress peak (106.5 MPa) obtained when the probe head reaches its sublimation temperature. The fatigue life is defined by cyclic load between compression (σ_{max} = 106.5 MPa) and unload (σ_{min} = 0 MPa), leading to an R = 0, and a stress ratio $S = \sigma_{compression}/\sigma_{max}$ = 106.5/170 = 0.63. Following the experimental fatigue life curves presented by Eto et al. [21] (Figures 9a) and 10a) of the cited contribution) for a similar graphite, FILD is expected to last > 10^5 cycles under these extreme conditions. The detector performs a few hundreds of cycles per year, and it can be easily replaced at the end of every campaign if needed. Therefore, it can be safely concluded that the probe head will not show fatigue-related damage.

5. **Conclusions**

A series of thermo-mechanical finite elements simulations have been performed to determine the limits of a magnetically driven fast-ion loss detector, and to prove the compatibility of the graphite probe head with radial scans. The sublimation temperature has been found to be the graphite probe head limit,

setting the upper boundary on the operational time of this detector. This will be used as one of the boundary conditions on an in-development real time closed-loop control system. Thermal simulations show that the probe head is far from the sublimation temperature during normal. The probe head is not expected to suffer fatigue even under the most extreme conditions.

The model shows its applicability for the rest of the FILD systems in AUG, expanding their operational window. The temperature and stress distribution of other plasma facing components in other tokamaks can be determined through the usage of the presented model. Magnetically driven diagnostics are compatible with future long-pulsed tokamaks or stellarators, where the system needs to be retracted during the shot. The presented model can be used to determine the operational windows and the boundary conditions on the control systems of these next-generation diagnostics.

6. **Acknowledgement**

This work has been carried out within the framework of the EUROfusion Consortium and has received funding from the Euratom research and training programme 2014-2018 and 2019-2020 under grant agreement No 633053. The views and opinions expressed herein do not necessarily reflect those of the European Commission.

7. **Bibliography**

[1] S. J. Zweben, R. Boivin, S. L. Liew, D. K. Owens, J. D. Strachan, and M. Ulrickson, "Constraints on escaping alpha particle detectors for ignited tokamaks," *Rev. Sci. Instrum.*, vol. 61, no. 11, pp. 3505–3508, Nov. 1990, doi: 10.1063/1.1141559.

[2] M. García-Muñoz, H.-U. Fahrbach, and H. Zohm, "Scintillator based detector for fast-ion losses induced by magnetohydrodynamic instabilities in the ASDEX upgrade tokamak," *Rev. Sci. Instrum.*, vol. 80, no. 5, p. 53503, May 2009, doi: 10.1063/1.3121543.

[3] R. K. Fisher *et al.*, "Scintillator-based diagnostic for fast ion loss measurements on DIII-D," *Rev. Sci. Instrum.*, vol. 81, no. 10, pp. 1–4, 2010, doi: 10.1063/1.3490020.

[4] J. F. Rivero-Rodriguez *et al.*, "A rotary and reciprocating scintillator based fast-ion loss detector for the MAST-U tokamak," *Rev. Sci. Instrum.*, vol. 89, no. 10, pp. 3–6, 2018, doi: 10.1063/1.5039311.

[5] M. Garcia-Muñoz *et al.*, "Convective and Diffusive Energetic Particle Losses Induced by Shear Alfvén Waves in the ASDEX Upgrade Tokamak," *Phys. Rev. Lett.*, vol. 104, no. 18, p. 185002, May 2010, doi: 10.1103/PhysRevLett.104.185002.

[6] J. Gonzalez-Martin *et al.*, "First measurements of a scintillator based fast-ion loss detector near the ASDEX Upgrade divertor," *Rev. Sci. Instrum.*, vol. 89, no. 10, pp. 2–7, 2018, doi: 10.1063/1.5038968.

[7] J. Galdon-Quiroga *et al.*, "Velocity space resolved absolute measurement of fast ion losses induced by a tearing mode in the ASDEX Upgrade tokamak," *Nucl. Fusion*, vol. 58, no. 3, 2018, doi: 10.1088/1741-4326/aaa33b.

[8] J. Gonzalez-Martin *et al.*, "First measurements of a magnetically driven fast-ion loss detector on ASDEX Upgrade," *J. Instrum.*, vol. 14, no. 11, 2019, doi: 10.1088/1748-0221/14/11/C11005.

[9] J. Gonzalez-Martin *et al.*, "Self-adaptive diagnostic of radial fast-ion loss measurements on the ASDEX Upgrade tokamak (invited)," *Rev. Sci. Instrum.*, vol. 92, no. 5, p. 053538, 2021, doi: 10.1063/5.0043756.

[10] J. Ayllon-Guerola *et al.*, "Dynamic and thermal simulations of a fast-ion loss detector for ITER," *Fusion Eng. Des.*, vol. 123, pp. 807–810, 2017, doi: 10.1016/j.fusengdes.2017.04.071.

[11] M. Rodriguez-Ramos *et al.*, "First absolute measurements of fast-ion losses in the ASDEX Upgrade tokamak," *Plasma Phys. Control. Fusion*, vol. 59, no. 10, 2017, doi: 10.1088/1361-6587/aa7e5f.

[12] R. Mitteau, A. Moal, J. Schlosser, and D. Guilhem, "Heat flux deposition on plasma-facing components using a convective model with ripple and Shafranov shift," *J. Nucl. Mater.*, vol. 266, pp. 798–803, 1999, doi: 10.1016/S0022-3115(98)00843-5.

[13] T. Eich *et al.*, "Inter-ELM Power Decay Length for JET and ASDEX Upgrade: Measurement and Comparison with Heuristic Drift-Based Model," *Phys. Rev. Lett.*, vol. 107, no. 21, p. 215001, Nov. 2011, doi: 10.1103/PhysRevLett.107.215001.

[14] T. Lunt *et al.*, "Near- And far scrape-off layer transport studies in detached, small-ELM ASDEX upgrade discharges by means of EMC3-EIRENE," *Plasma Phys. Control. Fusion*, vol. 62, no. 10, 2020, doi: 10.1088/1361-6587/aba9ff.

[15] B. Sieglin *et al.*, "Real time capable infrared thermography for ASDEX Upgrade," *Rev. Sci. Instrum.*, vol. 86, no. 11, p. 113502, Nov. 2015, doi: 10.1063/1.4935580.

[16] D. Silvagni *et al.*, "Scrape-off layer (SOL) power width scaling and correlation between SOL and pedestal

gradients across L, i and H-mode plasmas at ASDEX Upgrade," *Plasma Phys. Control. Fusion*, vol. 62, no. 4, 2020, doi: 10.1088/1361-6587/ab74e8.

[17] P. C. Stangeby, "A three-dimensional analytic model for discrete limiters in ITER," 2010, doi: 10.1088/0029-5515/50/3/035013.

[18] Ansys, "Ansys mechanical: Finite element analysis software," 2021. https://www.ansys.com/products/structures/ansys-mechanical.

[19] G. Glockler, "The Heat of Sublimation of Graphite and the Composition of Carbon Vapor," *J. Chem. Phys.*, vol. 22, no. 2, pp. 159–161, Feb. 1954, doi: 10.1063/1.1740023.

[20] A. Herrmann, R. Drube, T. Lunt, and P. De Marné, "Real-time protection of in-vessel components in ASDEX Upgrade," *Fusion Eng. Des.*, vol. 86, no. 6–8, pp. 530–534, 2011, doi: 10.1016/j.fusengdes.2011.02.037.

[21] M. Eto, T. Arai, and T. Konishi, "The fatigue strength of graphite and carbon materials for HTTR core components," *JAERI-Research*, vol. 98–024, no. March, 1998.